Baroclinic Wave Drag and Barotropic to Baroclinic Energy Transfer at Sills as Evidenced by Tidal Retardation, Seiche Damping and Diapycnal Mixing in Fjords

Anders Stigebrandt

Department of Oceanography, Earth Sciences Center, Göteborg University, Göteborg, Sweden

Abstract. Fluctuating barotropic flow over sills in stratified water is subjected to baroclinic wave drag and accompanying barotropic to baroclinic energy transfer. In fjords, this process has notable consequences, for instance, tidal retardation across fjord sills, damping of barotropic seiches and enhanced diapycnal mixing in the basin water. These may be computed from simple models only including local conditions in the sill area. This has been done for numerous fjords with quite satisfactory results as reviewed in this paper. It is therefore concluded that baroclinic wave drag and barotropic to baroclinic energy transfer only depend upon local conditions in the sill area.

Energy transferred from the barotropic tide to baroclinic motions at sills is eventually dissipated by turbulence and diapycnal mixing. If radiated away from the sill by progressive internal waves, the energy may be transferred to turbulence in places remote from the sill. Radiation of baroclinic energy from fjord sills, however, is often less than the energy gain by baroclinic wave drag, so there also seems to be a possibility for a short spatial pathway to dissipation and mixing close to the sill. It is suggested in this paper that the magnitude of the radiated fraction is regulated by the capacity of the fjord basin to dissipate internal waves. In a fjord with small capacity to dissipate internal waves, much of the baroclinic energy gained at the sill has to dissipate close to the sill.

The power for diapycnal mixing in most fjord basins is mainly derived from barotropic tides by baroclinic wave drag at sills. Diapycnal mixing in the abyssal ocean is probably driven in a similar way by baroclinic wave drag at bumps, sills, and ridges on the sea bottom. By analogy with the case in fjords, the energy transfer should be computed using local models. Furthermore, some of the transferred energy probably dissipates close to the topography and the rest is radiated away by internal waves and dissipated in remote places. The total mixing should thus be greater than the mixing related to the field of internal waves sustained by radiation from the topography. Estimates of the total diapycnal mixing in the abyssal ocean should therefore be based on observations covering the whole water column down to the seabed as also suggested by recently published dissipation profiles from the ocean.

1. Introduction

Growing evidence suggests that tides provide much of the power for mixing and the accompanying vertical circulation of the deep ocean, e.g., *Munk* (1966), *Sjöberg and Stigebrandt* (1992) and *Munk and Wunsch* (1998). The vertical mixing is coupled to tides by baroclinic wave drag acting on barotropic tides at sills, bumps and ridges in the bottom, e.g., *Cox and Sandström* (1962), *Bell* (1975) and *Sjöberg and Stigebrandt* (1992). Theoretical estimates of tidal mixing so far largely lack observational verification for the deep ocean. However, recent observations of dissipation in the abyssal ocean show the expected intensification close to rough topography, e.g. *Polzin et al.* (1997).

Physical processes are much easier to study in fjords than in the deep ocean, thus fjords often are suitable as ocean process laboratories. Basic knowledge of physical processes obtained from fjord studies may then be applied to other parts of the ocean. As an example, it may be mentioned that the model by *Sjöberg and Stigebrandt* (1992) is based on results essentially from fjord studies. Energy release from barotropic tides by baroclinic wave drag and pathways of the energy to turbulent dissipation and diapycnal mixing, the focal points of the present paper, might be partly different in the deep ocean and in fjords. Nevertheless, it is believed that elucidation of the mechanics of these processes in fjords might be quite helpful in developing an understanding of the way similar processes work in the deep ocean. The objective of the present paper is to summarize knowledge, gained from work on fjords during the last decades, about barotropic to

baroclinic energy transfer at sills and pathways of the energy to turbulent dissipation and diapycnal mixing.

Barotropic to baroclinic energy transfer at fjord sills due to baroclinic wave drag acting on time-dependent barotropic currents has been modeled with different kinds of stratification and sill topography. The models discussed in the present paper are local in the sense that only conditions in the immediate neighborhood of the sill are invoked. The models may be tested by comparison between predicted and observed estimates of the quantities listed below, which under certain circumstances only are due to baroclinic wave drag (see also Fig. 1).

1. Tidal response in fjords; retardation and amplitude reduction (section 3 below).
2. Damping of barotropic seiches in fjords (section 3).
3. Diapycnal mixing in the basin water of fjords (section 4).
4. Radiation of internal waves from sills in fjords (section 5).

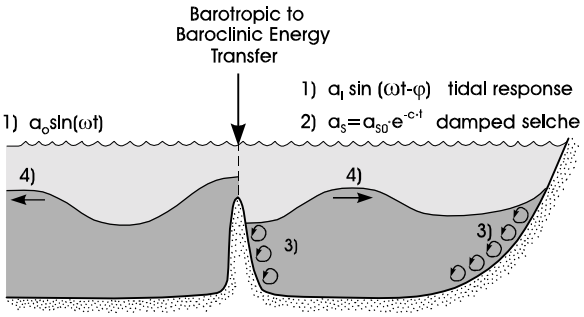

Figure 1. Consequences of baroclinic wave drag and barotropic to baroclinic energy transfer at sills in the mouth of fjords: (1) Tidal response in fjords, (2) damping of barotropic seiches, (3) diapycnal mixing in the basin, and (4) radiation of internal waves from the sill.

It seems that large-scale topographic drag and baroclinic wave drag are mutually exclusive processes in straits, occurring for supercritical and subcritical conditions, respectively. Baroclinic wave drag is the dominating drag acting on barotropic tidal flow in the mouth of most subcritical fjords. It is thus usually much greater than drag due to bottom friction. Baroclinic wave drag was introduced in a model for barotropic strait flow in *Stigebrandt* (1999). The model explains the observed tidal retardation in fjords where baroclinic wave drag is the dominating resistance to the barotropic flow. *Parsmar and Stigebrandt* (1997) used the same formulation for barotropic to baroclinic energy transfer at fjord sills to derive the damping coefficient of barotropic seiches in fjords. Their model explained the observed damping of the fundamental barotropic seiche in the Gullmar Fjord. As further discussed in the present paper, these cases verify that simple, local models describe barotropic to baroclinic energy transfer at sills due to baroclinic wave drag quite well.

From work on a large number of fjords, it is known that the vertical mixing and circulation of the basin water in fjords is driven mainly by barotropic to baroclinic energy transfer at fjord sills. Examples may be found in, for example, *Stigebrandt* (1976), *Stigebrandt and Aure* (1989), *Simpson and Rippeth* (1993), and *Tinis* (1995. There is an almost constant ratio between the rate of work done by turbulence against the buoyancy forces in the basin water and the energy transfer from barotropic to baroclinic motions at sills as estimated from the simple local models. The fact that the ratio is constant for a wide range of fjords shows that physical dimension and form of a fjord basin are of little or no importance for the energy transfer. A tracer experiment conducted in the Oslo Fjord indicates that dissipation takes place along the rim of the fjord basin, suggesting that energy derived from baroclinic wave drag be dissipated to turbulence close to the sea bottom. This may occur near the sill as well as remotely from the sill by interaction between internal waves and the sea bottom.

The observed radiation of baroclinic energy from fjord sills varies from almost 100% to less than 50% of the energy transfer from the barotropic tide via baroclinic wave drag as estimated by simple models. This suggests that there may be substantial dissipation of tidal energy already close to the sill in many fjords. Radiation of baroclinic energy from a fjord sill is thus generally less than the baroclinic energy gain at the sill. It is suggested in this paper that the magnitude of the radiated fraction should depend on the capacity of the fjord to dissipate internal waves. In a fjord with small capacity to dissipate internal waves (maybe due to highly reflecting side boundaries), much of the energy released by baroclinic wave drag at the sill should accordingly dissipate close to the sill. It was suggested in the preceding paragraph that the physical dimension and form of a fjord basin do not influence the process of baroclinic wave drag. However, physical dimension and form seem to influence radiation of internal waves from sills and thereby the spatial distribution of turbulent dissipation in a fjord basin.

This paper describes observed consequences of baroclinic wave drag and barotropic to baroclinic energy transfer at fjord sills. The theoretical framework for the analysis is given is section 2 where a simple local model for baroclinic wave drag and barotropic to baroclinic energy transfer in subcritical fjords is presented together with some derived consequences of this. In section 3 the simple local model to estimate barotropic to baroclinic energy transfer is verified using data for tidal phase shift from three fjords and the observed damping of the barotropic seiche in one fjord. In section 4 the extensive empirical evidence for tidally forced mixing in the basin water of fjords is presented. The relationship between barotropic to baroclinic energy transfer at fjord sills and

radiation of baroclinic energy into fjords is discussed in section 5. The paper is concluded in section 6 where a number of remaining research questions are asked.

2. Theoretical Framework and Methods

To demonstrate the mechanics of baroclinic wave drag and barotropic to baroclinic energy transfer one may use the simplest possible case, a two-layer stratification with the interface at sill depth. This is actually often a quite good approximation of real fjord stratification because particularly dense water that occasionally refills the basin is trapped by the sill. To keep the discussion simple one may consider the mouth of the fjord to be a rectangular strait of width B, length L and depth h. The velocity of the time dependent barotropic current through the strait is U_S(t).

From basic principles, the momentary rate of energy loss for barotropic flow between two basins, separated by a relatively narrow strait, is

$$\varepsilon = Qg\rho\Delta\eta \qquad (1)$$

The flow rate $Q=U_SBh$ has the same sign as $\Delta\eta = h_o - h_i$, h_o (h_i) is the time-dependent sea level in the outer (inner) basin, g the acceleration of gravity, and ρ the density of water. For Eq. (1) to be valid, the barotropic velocities both far upstream and far downstream of the strait have to be small (narrow strait). No essential dynamics are lost by this restriction.

Equation (1) does not reveal, or depend on, the nature of the energy loss and should apply independently of the details of the flow in and around the strait. From time series of Q and $\Delta\eta$, this equation may be used in a diagnostic way to compute the dissipation of barotropic strait flows. However, to study the mechanics of the energy loss a dynamic model for the flow in and around the strait is needed as discussed later in this section.

The following volume budget is applicable to a land-locked basin inside a strait:

$$A_i = \frac{dh_i}{dt} = Q + Q_f \qquad (2)$$

Here A_i is the horizontal surface area and Q_f the freshwater supply. This equation can be used to compute the barotropic transport from observed time series of h_i and Q_f. For the discussions of baroclinic wave drag in the present paper, possible complications due to freshwater supply, which usually varies on a much longer time scale than tides, will not be considered and thus Q_f will be considered negligible.

If tidal energy is not dissipated in the fjord, co-oscillating barotropic tides should take the shape of standing waves. However, if dissipation occurs, progressive barotropic tidal wave components will appear supporting the energy required by dissipation. The presence of progressive tidal components means that the phase of the tide increases up-fjord. As already mentioned above, the rate of dissipation of a tidal component may be estimated in a diagnostic way from Eq. (1), provided measurements of h_o and h_i are available. By guessing the functional form of the tidal response h_i in the land-locked basin, an analytic diagnostic relationship between the mean rate of dissipation and the tidal phase shift in the fjord may be derived as discussed below.

2.1 The diagnostic method to estimate tidal dissipation from sea level records

Putting $h_o = a_o \sin(\omega t)$ and assuming that the response in the land-locked basin is $h_i = a_i \sin(\omega t - \varphi)$, the transport Q may be expressed as a function of h_i using Eq. (2) with $Q_f = 0$. The relationship between a_o, a_i and the phase angle φ is readily found to be $a_i = a_o \cos(\varphi)$. Inserting in the expression for momentary dissipation, Eq. (1), and averaging over one tidal cycle, the following expression for the mean dissipation E_{av} may be obtained:

$$E_{av} = \frac{1}{4}\rho g A_i \omega a_o^2 \sin(2\varphi) \qquad (3)$$

From harmonic analysis of two time series, h_o and h_i, obtained outside and inside the strait, respectively, one may estimate a_o and φ for the component of frequency ω. Then the mean dissipation of the constituent is directly given by Eq. (3). As can be seen from this equation, maximum dissipation occurs when the phase lag in the land-locked basin equals 45^o. The amplitude a_i in the land-locked basin then equals $a_o/2^{1/2}$. This diagnostic method to estimate tidal dissipation from the tidal phase shift has been discussed by a number of authors, for example, *McClimans* (1978), *Farmer and Freeland* (1983), *Stacey* (1984), *Tinis* (1995). The very simple derivation above was presented by *Stigebrandt* (1999) who also showed that the linear response assumed in the derivation of Eq. (3) is consonant with baroclinic wave drag as further discussed below. As already stressed, the diagnostic method may be used to estimate tidal dissipation from sea level records but it does not reveal the nature of the energy loss. To do this, one needs a dynamic model describing the different drag forces and the accompanying energy losses acting on the barotropic current in the strait.

2.2 A dynamic model for barotropic flow in straits with baroclinic wave drag

There are three classes of resistance to barotropic flow causing energy losses in sea straits. Friction against the seabed transfer energy to turbulence in a bottom boundary layer. Large-scale barotropic form drag, caused by contraction-expansion induced by the ends of straits having smaller vertical cross-sectional areas than the adjacent basins, transfer energy to large-scale eddies in the expanding current downstream of the strait. These two kinds of flow resistance have been used frequently in strait

models for barotropic flow, e.g., *Stigebrandt* (1980). Baroclinic wave drag transfer barotropic energy to baroclinic waves in the stratified adjacent basins. To the best of the present author's knowledge, baroclinic wave drag was implemented in a strait flow model for the first time in *Stigebrandt* (1999) where the simple model presented below was derived.

The rate of energy loss suffered by barotropic flow in a rectangular strait, due to these three kinds of resistance, can be described by the expressions given in Eqs. (4), (5) and (6) below. If C_D is the drag coefficient for flow over the seabed and $A_s \approx BL$ the surface area of the strait bed, the rate of frictional energy loss in the strait is

$$\varepsilon_f = \rho C_D U_S^2 BL|U_S| \tag{4}$$

The rate of energy loss due to large-scale barotropic form drag is

$$\varepsilon_a = \frac{\rho}{2} U_S^2 Bh|U_S| \tag{5}$$

For a two-layer stratification the momentary transfer of barotropic energy to baroclinic waves in a stratified basin bordering the strait is

$$\varepsilon_w = \rho \frac{d}{h+d}|U_S| c_g Bh|U_S| \tag{6}$$

Here h, ρ_1, u_1 (d, ρ_2, u_2) are thickness, density and orbital velocity of the upper (lower) layer. The internal wave with group velocity c_g has the property that $hu_1=du_2$ and from the boundary condition of no flow through the sill one obtains $u_1=U_S\, d/(h+d)$, see *Stigebrandt* (1976, 1999) for further discussion of ε_w. It should be noted that Eq. (6) gives the barotropic to baroclinic energy transfer at one end of the strait. The total barotropic to baroclinic energy transfer at a strait is usually about twice ε_w because baroclinic wave drag operates at both ends of the strait. However, the magnitude of the two contributions may differ because d and c_g may be different in the two basins bordering the strait.

In Eq. (6) U_S^2 has been expressed as $|U_S|$ times $|U_S|$ to obtain similarity with Eqs. (4) and (5). The quantities multiplying the final $|U_S|$ in Eqs. (4), (5) and (6) are the drag forces due to bed friction, large-scale topographic drag and baroclinic wave drag, respectively. The baroclinic wave drag force was also discussed in *Sjöberg and Stigebrandt* (1992). Using Eqs. (4), (5) and (6) it is easy to estimate the relative magnitude of the three drag forces. It may be interesting to note that large-scale topographic drag dominates over bottom frictional drag if $h/L>2C_D$ (supercritical flows) and baroclinic wave drag dominates over bottom frictional drag if $h/L>\{C_D U_S (h+d)/(2c_g h)\}$ (subcritical flows).

In the derivation of Eq. (6), the kinematic boundary condition of no flow through the sill (i.e., the end wall of the fjord at the strait) is satisfied by the barotropic plus the only baroclinic wave mode. A prerequisite for this is that $F_t<1$ (wave basin - subcritical). Here the Froude number F_t equals U_{Sm}/c_g and U_{Sm} is the amplitude of the fluctuating barotropic current in the strait. If $F_t>1$ (jet basin - supercritical) it is assumed that the baroclinic wave drag at the ends of the strait is replaced by large-scale topographic drag developing a jet on the lee side of the strait. The demarcation value between jet and wave generation does not seem to be very sharp and internal waves appear to be generated also for F_t slightly greater than 1, e.g., *Blackford* (1978). However, this will not be discussed further in the present paper but see also a comment in the last paragraph of section 4 below.

Using Eqs. (4), (5) and (6) it is now possible to describe the total energy loss suffered by barotropic flow through a strait. In this paper only a short strait ($\varepsilon_f \ll \varepsilon_w$) with $F_t<1$ (i.e., $\varepsilon_a = 0$) is discussed for which one obtains $\varepsilon = 2\varepsilon_w$ if the barotropic to baroclinic energy transfers are equally large at the two ends of the strait. It is further assumed that $Q_f = 0$. Eqs. (1), (2) and (6) then give the following relationship between the momentary flow through the strait and sea level difference

$$Q = \frac{g\Delta\eta}{2c_g} \frac{Bh(D+H)}{d} \tag{7}$$

According to this equation, transports through straits are proportional to $\Delta\eta$ if the drag force is due only to baroclinic wave drag. Just for comparison it may be mentioned that if $\varepsilon = \varepsilon_a + \varepsilon_f$ the flow Q through the strait becomes proportional to the square root of $\Delta\eta$, see e.g., *Stigebrandt* (1980) for a discussion of this case including also effects of non-zero values of Q_f.

2.3 Damping of a barotropic seiche by baroclinic wave drag

Equation (6) was used in *Stigebrandt* (1976) and in *Parsmar and Stigebrandt* (1997) to discuss the damping of barotropic seiches in a rectangular fjord with a node in the mouth. If E is the energy of the seiche, the damping coefficient C of the seiche is defined by

$$C = -\frac{1}{E}\frac{dE}{dt} \tag{8}$$

If the damping is due to baroclinic wave drag at the fjord sill one obtains

$$\frac{dE}{dt} = -2\varepsilon_w \tag{9}$$

Here ε_w is given by Eq. (6) and for simplicity it is assumed that the barotropic to baroclinic energy transfers are equally large at both ends of the strait. The energy of

the fundamental (quarter-wave) barotropic seiche is readily found to be, see e.g., *Parsmar and Stigebrandt* (1997),

$$E = \frac{1}{4}\rho g a_i^2 A_f \tag{10}$$

Here a_i is the amplitude of the seiche at the head of the fjord of area A_f. Using Eqs. (6), (8), (9) and (10) one may obtain the following analytical expression for the damping coefficient

$$C = \frac{16 d \omega^2 A_f}{\pi^2 g(d+h)Bh} c_g \tag{11}$$

For a discussion of this expression and an estimate of the neglected bottom friction, see *Parsmar and Stigebrandt* (1997).

2.4 Diapycnal mixing in fjord basins driven by barotropic to baroclinic energy transfer

It was suggested in *Stigebrandt* (1976) that most of the diapycnal mixing in the Oslo Fjord is performed by dissipating internal tides generated at the sill in the mouth of the fjord. The time mean barotropic to baroclinic energy transfer, obtained from Eq. (6), is given by

$$E_w = \rho_0 \frac{A_i^2 a_i^2 \omega^2 d}{Bh(h+d)} c_g \tag{12}$$

Here a_i is the amplitude in the fjord of the tidal component of frequency ω. Diapycnic mixing in the basin water is sustained by turbulent dissipation ε_d. The relationship between the rate of work against the buoyancy forces due to diapycnic mixing and dissipation is

$$\int_V \kappa N^2 dV = Rf\,\varepsilon_d \tag{13}$$

Here $\kappa = \kappa(z)$ is the horizontal and time (over one tidal cycle) mean vertical diffusivity, $N=N(z)$ is the buoyancy frequency, z the vertical coordinate, V the volume of the basin water and Rf is the efficiency of turbulence with respect to irreversible (diapycnic) work against the buoyancy forces. It was argued in *Stigebrandt* (1976) that all the energy transferred from barotropic to baroclinic motions at the sill dissipates in the basin water. If this is the only energy source for turbulence and mixing in the basin water then $\varepsilon_d = E_w$. This is often a quite good approximation although some additional contributions to dissipation may be supplied by other energy sources, see *Stigebrandt and Aure* (1989). Rf should be tantamount to the Richardson flux number. The ratio Rf between the rate of work done against the buoyancy forces in the basin water and the barotropic to baroclinic energy transfer at the fjord sill is further discussed in section 4 below.

To evaluate the integral in Equation (13) one must know the horizontal mean vertical diffusivity $\kappa(z)$ and the buoyancy frequency $N(z)$. Using the so-called budget method, the horizontal mean vertical diffusivity may be evaluated from vertical profiles of salinity and temperature obtained at different times. The method requires that the basin water has been stagnant in the period between the recordings of the profiles so salinity and temperature changes only are due to vertical diffusion. By stagnant is thus meant that no advective water exchange has taken place in the period. The budget method is further discussed in, e.g., *Gade* (1970), *Gargett* (1984), and *Stigebrandt and Aure* (1989).

The fact that Rf is approximately constant in fjord basins, see section 4, means that Eq. (13) may be used to estimate κ for fjord basins where E_w can be computed from Eq. (12). This was done in *Stigebrandt and Aure* (1989) who empirically determined the distribution of turbulent dissipation as a function of the buoyancy frequency using data from a number of fjords. In this way, they estimated the following expression for κ

$$\kappa = \frac{w}{M^2 \rho_0} c \left(\frac{N}{M} \right)^{\delta} \tag{14}$$

Here w is the volume mean turbulent dissipation defined by $w = \varepsilon_d / V_b$, V_b the volume of the basin water, M the weighted average of N in the basin water, and c and δ are non-dimensional empirical constants depending on the shape of the vertical stratification. For most fjords, the vertical stratification was well behaved and for these cases it was found that $c \approx 1$ and $\delta \approx$ -1.5, see *Stigebrandt and Aure* (1989) for details. These fjord results were later used in *Sjöberg and Stigebrandt* (1992) to estimate the vertical variation of $\kappa(x,y,z)$ in the abyssal ocean from estimates of the barotropic to baroclinic energy transfer $E_w(x,y)$.

Local models for barotropic to baroclinic energy transfer due to baroclinic wave drag have also been developed for more complicated stratification, e.g., *Stigebrandt* (1980) and *Stacey* (1984). Finally, it should be noted that the bottom slope of sills in fjords usually is much greater than the critical slope. Direct generation of internal wave rays by sills is therefore probably not very important.

3. Baroclinic wave drag and barotropic to baroclinic energy transfer at fjord sills

The model for barotropic flow in straits with baroclinic wave drag as the only drag force, presented in section 2, can be used to compute the tidal response in fjords. Such computations offer a possibility to verify the model for barotropic to baroclinic energy transfer provided the tidal response in the fjord is known from observations. The model was applied in *Stigebrandt* (1999) to three fjords for which the phase shift of semi-diurnal tides was known. With known sea level outside the sill, $h_o = a_o \sin(\omega t)$ and with $Q_f = 0$, Eqs. (2) and (7) were thus used to

compute the sea level h_i (t) in the fjords. The results for the three cases are discussed below.

The model was applied to the inner Oslo Fjord for which A_f= 200 km^2, B = 600 m, h = 15 m, d = 65 m, c_g = 0.8 m s^{-1}. The mouth (the Drøbak Strait) is extremely short and sea bed friction may be neglected (cf. *Stigebrandt*, 1976). A semidiurnal tide of amplitude 0.15 m is assumed to exist outside the fjord. Using these figures the model predicts that the dissipation is about 2 × 590 kW (internal waves emitted from both sides of the sill). The phase lag of the semidiurnal tide in the fjord is predicted to be 22°. This is independent of the amplitude as long as F_t<*1* and Equation (7) applies. The phase lag should thus be approximately the same for all semidiurnal components of the tide. For the computation it is assumed that the internal wave speed outside the sill equals that inside which probably is an overestimate since the stratification is weaker outside than inside the sill most of the time. Thus, the predicted phase shift of M_2 across the sill is probably overestimated by some degrees. The observed phase shift is about 15° (*Anonymous*, 1997).

The model was also applied to Knight Inlet where the inner sill has the width B = 1250 m and depth h=60 m while d = m and A_f= 220 km^2. The tidal component M_2 has the amplitude 1.5 m and for summertime stratification c_g = 0.83 (0.50) m s^{-1} for internal wave vertical mode 1 (2) (*Webb and Pond*, 1986). These authors report that the phase shift of M_2 across the inner sill in Knight Inlet is 2-3° and from time series of velocity and density at different depths in the fjord they find that the internal wave response is a mixture of vertical modes 1 and 2. *Stacey* (1984) estimated the dissipation inside the sill to about 7 MW under similar conditions of stratification. The present model predicts that the phase shift across the inner sill is 3° (2°) and the dissipation inside the sill is predicted to be 10.1 (5.8) MW for mode 1 (2) internal wave response. With a mixed mode 1 and 2 response, the model thus seems to predict the conditions in Knight Inlet rather well.

The Idefjord, denoted basin 2 in the computations below, is situated at the Skagerrak coast and constitutes part of the border between Sweden and Norway. The mouth of the Idefjord has two narrow (~70 m) and shallow (~9 m) sills, at a distance 1.2 km from each other, separated by a wider and deeper small basin (basin 1). It is expected that baroclinic wave drag acts at both sides of both sills as long as F_t<1. Baroclinic wave drag is then much greater than frictional drag. From *Munthe Kaas* (1970) one may obtain the following numbers: A_{f1} = 0.27 km^2, d_1 = 12 m, h_1 = 9 m, B_1 = 58 m, c_{g1} = 0.5 m s^{-1}, A_{f2} = .4 km^2, d_2 = 19 m, h_2 = 9.5 m, B_2 = 78 m, c_{g2} = 0.6 m s^{-1} where subscript 1 (2) refers to basin 1 (2). By simultaneously solving Equations (2) and (7) for basins 1 and 2 coupled in series one obtains for a semidiurnal tidal component a phase shift of 33° between the coastal water and the Idefjord, and the amplitude in the fjord is 83% of that in the coastal water. These results are very close to the observed phase shift (36°) and amplitude reduction in the fjord (*Parsmar*, personal communication, 1997).

The damping of the barotropic seiche in the Gullmar Fjord, Sweden, was studied by *Parsmar and Stigebrandt* (1997). They used the almost one-year-long sea level record from 1985 obtained at Bornö Hydrographical Station, situated in the inner part of the fjord, to estimate the damping coefficient of the barotropic seiche of period of about 2 hours. The seiche was described and modeled by *Zeilon* (1913). He also described observations of internal waves having the same frequency as the barotropic seiche in the Gullmar Fjord but did not discuss the damping of the seiche (*Zeilon*, 1912, 1913). Figure 2 shows monthly means of the theoretical, Eq. (11), and the observed damping coefficient in the Gullmar Fjord as estimated by *Parsmar and Stigebrandt* (1997). It can be seen that the two curves follow each other rather nicely in an annual cycle, caused by the varying vertical stratification, measured once a month the same year in the middle of the fjord (Fig. 3).

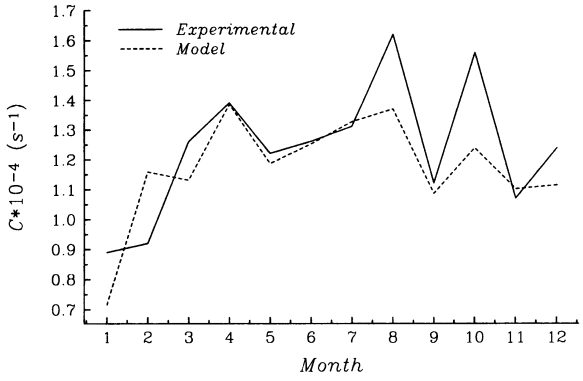

Figure 2. The annual cycle of modeled, Eq. (11), and observed (experimental) damping coefficient for the barotropic seiche in the Gullmar Fjord in 1985. (From *Parsmar and Stigebrandt*, 1997).

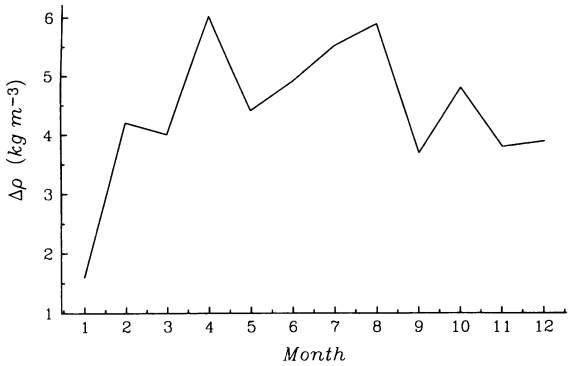

Figure 3. Monthly values of $\Delta\rho$ for a two-layer approximation of the stratification in the Gullmar Fjord in 1985. (From *Parsmar and Stigebrandt*, 1997).

It seems that the strait flow model with only baroclinic wave drag predicts the observed tidal phase shift quite well for strait flows with $F_t<1$ and $\varepsilon_f << \varepsilon_w$. From this, one may conclude that the baroclinic wave drag as implemented in the model seems to be quite realistic. In particular it is interesting to note that in spite of the short separation (1.2 km) between the sills in the mouth of the Ide Fjord, baroclinic wave drag is apparently fully developed at both sides of the two sills. The fact that the model for barotropic to baroclinic energy transfer also explains the observed damping of the seiche in the Gullmar Fjord further strengthens the conclusion that the process of baroclinic wave drag should be regarded as a locally controlled process and that the accompanying barotropic to baroclinic energy transfer is well estimated by Eq. (6). It is notable that in some of the studied cases the amplitude of the barotropic flow is near critical but still the linear model for barotropic to baroclinic energy transfer seems to perform well also for these cases.

4. Relationship between barotropic to baroclinic energy transfer and diapycnal mixing in fjord basins

It was suggested in *Stigebrandt* (1976) that most of the diapycnal mixing in the basin water of the Oslo Fjord is performed by dissipating internal tides generated at the sill in the mouth. Using data from this fjord the efficiency factor *Rf* of turbulent mixing processes was estimated to be about 0.05. *Stigebrandt and Aure* (1989) investigated the mixing efficiency in a large number of fjord basins in Norway. They found that the mixing efficiency equals about 0.056 in fjords where the amplitude of the barotropic current over the sill is subcritical (wave-basins). Figure 4 shows the observed rate of work against the buoyancy forces in the fjords, normalized by the horizontal area of the fjords at sill level, versus the theoretical

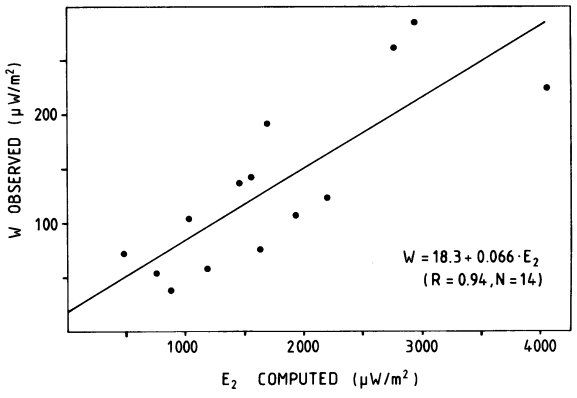

Figure 4. Observed normalized rate of work against the buoyancy forces in the basin water (*w observed*) versus the estimated barotropic to baroclinic energy transfer by semidiurnal tides (E_2 *computed*) at the sill for a number of fjords. (From *Stigebrandt and Aure*, 1989).

barotropic to baroclinic energy transfer. Studies in several other fjords confirm that the value of *Rf* is about 0.06, e.g., *Svensson* (1980), *Simpson and Rippeth* (1993) and *Tinis* (1995).

Based on investigations in a large number of fjords in Scandinavia, Scotland, and Canada, the mixing efficiency ratio *Rf* thus appears to be about constant and independent of the dimension and form of fjords. Not even the ratio between the volume of the basin water and the total fjord volume seems to have any importance. This supports the assumption, put forward in *Stigebrandt* (1976), that most of the energy released by baroclinic wave drag dissipates in the basin water. Even very short fjords, of lengths that are only small fractions of the wavelengths of internal tides, have the same efficiency ratio as large fjords. This must imply that the process of barotropic to baroclinic energy transfer by baroclinic wave drag at fjord sills should not be influenced by possible reflection of internal tides in the inner reaches of the fjord. This conclusion, implying that baroclinic wave drag is a process determined by the local conditions at the sill, was also drawn in section 3 above from the Ide Fjord case, where the two sills in the mouth separated by a basin only about 1.2 km long, were shown to give rise to full baroclinic wave-drag.

Guided by a simple laboratory experiment, the present author suggested that the baroclinic energy gained at sills by baroclinic wave drag is transferred to turbulence and mixing by the breaking of internal waves against sloping bottoms (*Stigebrandt*, 1976). From this one should expect to find high values of the vertical diffusivity along the rim of the fjord basin (hot spots in the terminology of *Munk*, 1997) and small values in the interior. A boundary-mixing model based on this scenario was described in *Stigebrandt* (1976). An experiment in the Oslo Fjord, with a tracer initially introduced in the interior of the basin water showed that diapycnal mixing in the interior really is much smaller than the basin average, see *Stigebrandt* (1979). This experiment supports the view that diapycnal mixing takes place close to the bottom, either by waves breaking against the bottom, or by wave-bottom interaction creating high local shear in the water column close to the bottom, or by turbulence generated close to the sill. To the best of the present author's knowledge no direct observations of the spatial distribution of turbulent dissipation or mixing in fjord basins have been published.

Stigebrandt and Aure (1989) also investigated the efficiency of diapycnal mixing in the basin water of supercritical so-called jet-fjords, where the amplitude of the barotropic tide over the sill exceeds the speed of internal waves in the fjord. The mixing efficiency for these cases defined by Eq. (13) with ε equal to the dissipation of the jet, varied a lot. The mean value was about 0.01, which is much lower than for wave basins. This is because the jet dissipates close to the sea surface and only little of the jet energy is transmitted to deeper layers. However, it seems that internal tides may be generated also in jet-fjords (*Tinis*, 1995, *Allen and Simpson*, 1998). Wave generation

should then not be the result of baroclinic wave drag but be due to a completely different mechanism with the fluctuating jet acting as a piston. Wave generation probably occurs in the vertical cross-section of the fjord where the speed of the declining jet has been reduced to the speed of the lowest internal wave mode.

5. Relationship between barotropic to baroclinic energy transfer at fjord sills and radiation of baroclinic energy into fjords

One might expect that the energy transferred from barotropic to baroclinic motions by baroclinic wave drag at fjord sills would radiate away from the sill by internal waves. If there is no dissipation at or near the sill one should be able to verify models for barotropic to baroclinic energy transfer from estimates of the power of the internal wave radiation. This expectation led the present author to estimate the radiation from the Dröbak sill in the Oslo Fjord. From sparse current measurements it was found that the seaward radiation was about 110% of the expected radiation while the landward radiation was about 80% (*Stigebrandt*, 1979). However, the estimate of the seaward radiation from the sill was considered uncertain because of uncertainty of the stratification. *De Young and Pond* (1989) found that radiation of baroclinic energy away from sills in some Canadian fjords was only 50%-80% of the expected radiation. Thus, it seems that there often is a substantial transfer of baroclinic energy to small-scale turbulence in or close to the sills (the short pathway).

The method to compute barotropic to baroclinic energy transfer under the assumption that barotropic and baroclinic modes together satisfy the boundary condition of vanishing normal velocity at non-horizontal topography seems to give quite adequate results for the energy transfer. Evidence based on tidal retardation (phase shift) in three fjords and damping of the barotropic seiche in one fjord was presented in section 3. Further evidence based on the observed constant and the relationship between barotropic and baroclinic energy transfer and the rate of diapycnal mixing in the basin water of fjords was presented in section 4. From all these cases it seems that vertical stratification and the large-scale topography of the sill (height, depth below the sea surface and width) and amplitude and frequency of the barotropic current over the sill are the only properties of the fjord that matter for the topographic barotropic to baroclinic energy transfer. There is no evidence for influence from the field of internal waves in the fjord. It thus appears that the barotropic to baroclinic energy transfer (and the baroclinic wave drag upon the barotropic current) at fjord sills should be considered to be a local process that can be estimated quite well from simple models. The internal wave response in the fjord, however, seems to differ from fjord to fjord.

From presently available information, it is here suggested that the internal wave response to the baroclinic forcing at the sill depends on the capacity of the fjord basin to dissipate internal waves. In basins with high dissipation capacity, most of the baroclinic energy provided by baroclinic wave drag at the sill may possibly be transmitted by progressive internal waves further into the fjord. In other fjords with low dissipation capacity, only little of the baroclinic energy provided at the sill may be transmitted into the fjord and the rest is dissipated close to the sill. If this view is correct, radiation of internal wave energy from sills is not a good measure of the barotropic to baroclinic energy transfer at sills. It should rather be a measure of the capacity of the inner reaches of a fjord to dissipate internal waves.

6. Concluding remarks

It has been shown that the barotropic to baroclinic energy transfer at fjord sills is well estimated by a simple local model for a large variety of basin conditions. From this, it is concluded that the process of baroclinic wave drag essentially is a local process determined by the topography of the sill, the amplitude and frequency of the fluctuating barotropic flow and the stratification in the fjord. The model applies equally well for a wide range of fjords so the magnitude and form of a fjord basin seem to be of no importance for the process of baroclinic wave drag. The model is based on the assumption that the boundary condition at the sill-fjord junction is satisfied by the barotropic flow together with progressive internal waves. From this, it might seem logical to verify the model by comparing modeled and observed radiation of internal waves from the sill. However, as discussed in the present paper, the net radiation of baroclinic energy into fjords seems to also depend on the capacity of the fjord basin to dissipate internal waves. Contrary to the baroclinic wave drag, the fjord capacity to dissipate internal waves is probably dependent on both the magnitude and form of the fjord basin. Thus, there should be no simple relationship between the barotropic to baroclinic energy transfer at the sill and the net transfer (radiation) of baroclinic energy into a fjord.

The pathways of energy gained by baroclinic wave drag at sills to turbulent dissipation and mixing in fjords are apparently complex. This suggests a number of future investigations to clarify the pathways. How is turbulent dissipation in fjords distributed in time and space? Particular care should be taken to obtain observations near areas of wave generation (sills) and along the rim of the basins where most of the mixing probably occurs. Which factors control the distribution of dissipation of internal waves in fjords? In this paper, it is suggested that the net radiation of internal wave energy into a fjord might be controlled by (and cannot exceed) the capacity of the fjord to dissipate internal waves. Having data from a wide range of fjords, it should be possible to find the key factors determining the capacity of a fjord to dissipate internal waves. As argued earlier in this paper, these key factors are probably related to physical dimension and form

of the fjord basin. By which mechanisms are internal waves dissipated close to sills in fjords where the barotropic to baroclinic energy transfer at the sill exceeds the capacity of the fjord to dissipate internal waves?

The closed character of fjord basins beneath the sill level during stagnant conditions gives an opportunity to estimate the efficiency *Rf* of turbulence with respect to mixing, using the energy budget in Eq. (13). The dominating energy source for the turbulent mixing processes in most fjord basins is due to baroclinic wave drag at the sill. There may also be energy contributions by other sources, which tend to overestimate *Rf* if not included in the energy budget. However, these other possible contributions are believed to be small in most fjords. If on the other hand, some of the energy gained by baroclinic wave drag is dissipated above sill level, *Rf* tends to be underestimated. Estimates in different wave fjords repeatedly give an efficiency of about 0.06. The present author believes that the estimate of *Rf* from fjord basins actually is the best estimate available in oceanography. However, in oceanographic literature one often uses $Rf = 0.2$ but evidence for this value seems obscure. Fjords are usually salt stratified while most parts of the ocean are dominated by temperature stratification. A possible difference in the mixing efficiency between waters stratified by salt and temperature respectively may then explain the different values of *Rf*. However, this issue should be investigated further.

Extrapolation of the fjord results to the ocean suggests that (1) barotropic to baroclinic energy transfer should be computed using local models and (2) the radiation of energy away from locations where it is released by baroclinic wave drag might be appreciably less than the barotropic to baroclinic energy transfer. Thus, a substantial part of the dissipation might take place close to the topography where baroclinic wave drag occurs. This was also pointed out in *Sjöberg and Stigebrandt* (1992). Recent observations of dissipation from the deep ocean show enhanced dissipation near the seabed in areas with strong bottom topography, e.g. *Polzin et al.* (1997).

How closely may ridges and bumps be situated to contribute to baroclinic wave drag? On might think that topography with horizontal length scales less than the wavelength of internal tides are unimportant. However, the idea that baroclinic wave drag is a local process and the examples from Ide Fjord and other fjords disprove this! Topographic features of even quite small horizontal length-scales probably contribute to baroclinic wave drag provided the surrounding water is stratified. Thus, small amplitude topography submerged in a homogeneous bottom boundary layer should not contribute very much to baroclinic wave drag.

Baroclinic wave drag on barotropic tides might be the major mechanism to support energy to turbulence and mixing in the deep ocean. However, the contribution by winds is so far not clear, see estimates by e.g., *Kundu* (1993), *Nilsson* (1995) and *Munk and Wunsch* (1998). An attempt to investigate purely wind-driven mixing beneath the surface layers is presently undertaken in the virtually tide-less Baltic proper by the multinational experiment DIAMIX. High-resolution measurements of currents, density and dissipation will be made during two-week periods in summer and winter. The objective is to describe and parameterize the purely wind-driven mixing of the Baltic proper deepwater. A future goal is to generalize this parameterization and apply it to the open ocean for a comparison between wind-driven and tidally driven mixing. An investigation using the budget method and historic hydrographic data from the Baltic has recently been made by *Axell* (1998) who found a strong seasonal variation in mixing intensity in pace with the wind forcing.

Acknowledgments. This work was supported by the Swedish Natural Science Research Council (NFR). The author wants to thank Peter Müller for the invitation to participate in the 'Aha Huliko'a Workshop on Internal Wave Modeling.

References

Allen, G.L. and J.H. Simpson, Reflection of the internal tide in the upper Loch Linnhe, a Scottish Fjord. *Estuarine, Coastal Shelf Sci., 46*, 683-701, 1998.

Anonymous, Tidevannstabeller (Tide Tables) for den norske kyst. *Statens Kartverk, Sjökarteverket, Norway*, 80 pp., 1997 [Available from Sjökarteverket, Box 36, N-4001 Stavanger, Norway].

Axell, L., On the variability of Baltic Sea deepwater mixing. *J. Geophys. Res., 103*, 21667-21682, 1998.

Bell, T.H. Jr., Topographically generated internal waves in the open ocean. *J. Geophys. Res., 80*, 320-327, 1975.

Blackford, B.L., On the generation of internal waves by tidal flow over a sill – a possible nonlinear mechanism. *J. Mar. Res., 36*, 529-549, 1978.

Cox, C. and H. Sandström, Coupling of internal and surface waves in water of variable depth. *J. Oceanog.l Soc. Jpn, 20*, 499-513, 1962.

De Young, and S. Pond, Partition of energy loss from the barotropic tide in fjords. *J. Phys. Oceanogr., 19*, 246-252, 1989.

Farmer, D.M. and H. Freeland, The physical oceanography of fjords. *Prog. Oceanog., 12*, 147-220, 1983.

Gade, H.G., Hydrographic investigations in the Oslofjord: A study of water circulation and exchange processes. *Rep. 24. Geophys. Inst. Div. A, Univ. of Bergen, Norway*, 193 pp. + figs., 1970

Gargett, A.E., Vertical eddy diffusivity in the ocean interior. *J. Mar. Res., 42*, 359-393, 1984.

Kundu, P.K., On internal waves generated by travelling wind. *J. Fluid Mech., 254*, 529-560, 1993.

McClimans, T.A., On the energetics of tidal inlets to land-locked fjords. *Mar. Sci. Commun., 4*, 121-137, 1978.

Munk, W., Abyssal recipes. *Deep-Sea Res., 13*, 707-730, 1966.

Munk, W., Once again: once again – tidal friction. *Prog. Oceanog. 40*, 7-35, 1997.

Munk, W. and C. Wunsch, Abyssal recipes II: energetics of tidal and wind mixing. *Deep-Sea Res. I, 45*, 1977-2010, 1998.

Munthe Kaas, H., Iddefjorden og dens forurensningsproblemer. Rapp. Nr. 2: Situasjonsrapport pr. 1 desember 1969. *NIVA, Oslo, Rep. O-113/64*. 33 pp., 1970 [Available from NIVA, Box 173 Kjelsås, N-0411 Oslo, Norway]

Nilsson, J., On the energy flux from travelling hurricanes to the oceanic internal wave field. *J. Phys. Oceanogr., 25*, 558-573, 1995.

Parsmar, R. and A. Stigebrandt, Observed damping of barotropic seiches through baroclinic wave drag in the Gullmar Fjord. *J. Phys. Oceanogr., 27*,849-857, 1997

Polzin, K.L., J. M. Toole, J.R. Ledwell, and R.W. Schmitt, Spatial variability of turbulent mixing in the abyssal ocean. *Science, 276*, 93-96, 1997.

Simpson, J.H. and T. Rippeth, The Clyde Sea: a model of the seasonal cycle of stratification and mixing. *Estuarine Coastal Shelf Sci., 37*, 129-144, 1993.

Sjöberg, B. and A. Stigebrandt, Computations of the geographical distribution of the energy flux to mixing processes via internal tides: its horizontal distribution and the associated vertical circulation in the ocean. *Deep-Sea Res., 39*, 269-291, 1992.

Stacey, M.W., The interaction of tides with the sill of a tidally energetic inlet. *J. Phys. Oceanogr., 14*, 1105-1117, 1984.

Stigebrandt, A., Vertical diffusion driven by internal waves of tidal origin in a sill fjord. *J. Phys. Oceanogr., 6*, 486-495, 1976.

Stigebrandt, A.. Observational evidence for vertical diffusion driven by internal waves of tidal origin in the Oslofjord. *J. Phys. Oceanogr., 9*, 435-441, 1979.

Stigebrandt, A., Some aspect of tidal interaction with fjord constrictions. *Estuarine Coastal Mar. Sci., 13*, 197-211, 1980.

Stigebrandt, A., Resistance to barotropic tidal flow in straits by baroclinic wave drag. *J.Phys. Oceanogr., 29*, 191-197, 1999.

Stigebrandt, A. and J. Aure, Vertical mixing in the basin waters of fjords. *J. Phys. Oceanogr., 19*, 917-926, 1989.

Svensson, T., Tracer measurement of mixing in the deep water of a small, stratified sill fjord, in *Fjord Oceanography* (H.J. Freeland, D.M. Farmer and C.D. Levings, Eds.). Plenum Press. P. 233-240, 1980.

Tinis, S.W., The circulation and energetics of the Sechelt Inlet System, British Columbia. PhD thesis, Dept, of Oceanography, the University of British Columbia, 173 pp, 1995 [Available from Dept. Of Earth and Ocean Sciences, the University of British Columbia, 6339 Stores Road, Vancouver, British Columbia V6T 1Z4].

Webb, A.J. and S. Pond, A modal decomposition of the internal tide in a deep, strongly stratified inlet: Knight Inlet, British Columbia. *J. Geophys. Res., 91*, 9721-9738, 1986.

Zeilon, N., On the tidal boundary waves and related hydrodynamical problems. *Kungl. Svenska Vetenskapsakademiens Handlingar, Vol. 47 (4)*, 46 pp, 1912.

Zeilon, N., On the seiches of the Gullmar Fjord. *Sven. Hydrogr. Biol. Komm. Skr*., V, 1-17, 1913.